

## Glass panes acting as shear wall

***Citation for published version (APA):***

Huveners, E. M. P., Herwijnen, van, F., Soetens, F., & Hofmeyer, H. (2007). Glass panes acting as shear wall. *Heron*, 52(1/2), 5-29.

***Document status and date:***

Published: 01/01/2007

***Document Version:***

Publisher's PDF, also known as Version of Record (includes final page, issue and volume numbers)

***Please check the document version of this publication:***

- A submitted manuscript is the version of the article upon submission and before peer-review. There can be important differences between the submitted version and the official published version of record. People interested in the research are advised to contact the author for the final version of the publication, or visit the DOI to the publisher's website.
- The final author version and the galley proof are versions of the publication after peer review.
- The final published version features the final layout of the paper including the volume, issue and page numbers.

[Link to publication](#)

***General rights***

Copyright and moral rights for the publications made accessible in the public portal are retained by the authors and/or other copyright owners and it is a condition of accessing publications that users recognise and abide by the legal requirements associated with these rights.

- Users may download and print one copy of any publication from the public portal for the purpose of private study or research.
- You may not further distribute the material or use it for any profit-making activity or commercial gain
- You may freely distribute the URL identifying the publication in the public portal.

If the publication is distributed under the terms of Article 25fa of the Dutch Copyright Act, indicated by the "Taverne" license above, please follow below link for the End User Agreement:

[www.tue.nl/taverne](http://www.tue.nl/taverne)

***Take down policy***

If you believe that this document breaches copyright please contact us at:

[openaccess@tue.nl](mailto:openaccess@tue.nl)

providing details and we will investigate your claim.

# Glass Panes Acting as Shear Wall

E.M.P. Huveners, F. van Herwijnen, F. Soetens, and H. Hofmeyer

Faculty of Architecture, Building and Planning, Structural Design Group, Technische Universiteit Eindhoven, Eindhoven, the Netherlands

The in-plane stiffness of glass panes can be mobilized to stabilize a steel framework e.g. in a façade. The brittle glass pane has to be structurally bonded to the framework and a circumferentially glued joint is then an appropriate technique. The joint type and adhesive determine the stress distribution in the pane and the horizontal displacement of the framework. Both criteria are important for stabilizing buildings: the stress distribution for determining the critical tensile stress (safety) and the displacement for serviceability. Three joint types are defined and two types of adhesive are investigated. Joint type 1 is a polyurethane joint on end, joint type 2 is a two-sided epoxy joint and joint type 3 is a one-sided epoxy joint. The systems have annealed float glass enclosed by a steel frame consisting of rigid elements. The systems are displacement controlled (horizontal) at the right top corner.

The load-displacement relation of systems with joint type 1 is bi-linear. The first part of the diagram shows low stiffness and the pane remains intact. The second part is stiffer, because of pane-frame contact at left bottom corner and at right top corner. The compressed diagonal of the pane transfers the load to the support. Hereafter, the pane gradually cracks at the corners of the compressed diagonal at increasing load and shows a good post-cracking behaviour. These systems are modelled as one strut model with effective width of one-third of the compressed diagonal.

The load-displacement relation of systems with joint type 2 shows a gradually decreasing stiffness at increasing load. The stiffness is clearly larger than the systems with joint type 1. The pane starts cracking at one of the bottom corners. Then the succeeding cracks are parallel to the compression diagonal. These cracks have small influences on the system. The final crack leads to a decrease of stiffness. The post-cracking behaviour of the systems is good, because after the first cracks occur, the pane resists more load. The principle stresses are regularly distributed at smaller loads, but larger compression stresses occur in the compressed diagonal at larger loads. These systems are modelled as shear wall.

The load-displacement relation of systems with joint type 3 also shows a gradually decreasing stiffness at increasing load. The stiffness is slightly smaller than systems of joint type 2. The first cracks start along the right mullion at the bottom. The final crack starts at the bottom of the left

mullion to the right top corner. These systems have no remaining capacity after failure. The principle stresses are regularly distributed and small, except for the left bottom corner. These systems are also modelled as shear wall.

*Key words: Glass pane, in-plane load, shear wall, glued joint*

## 1 Introduction

The glass façade of a building is an envelope structure consisting of glass panes, transoms and mullions. The façade is connected to the stable main bearing system of the building. The panes resist transversal loads e.g. wind, but are not loaded in-plane except by own weight, because the pane is freely enclosed (Figure 1, left). The in-plane stiffness of glass panes offers the possibility to use panes as stabilising elements. So, the façade's structure can be reduced to one integrated, structural layer (Figure 1, right), but the connection details have to be changed.

The idea to use glass panes as stabilising elements is not new. The 19<sup>th</sup> century green houses e.g. Bicton Garden in Dervin (UK) [2] are stable thanks to their glass panes. The small glass panes were bonded to the iron main bearing structure with putty. Nowadays, adhesives are used instead of putty. There are two advantages to use a glued joint connection between glass pane and framework. Firstly, a glued joint spreads stresses and secondly, it forms an interlayer to prevent direct glass-metal contact.

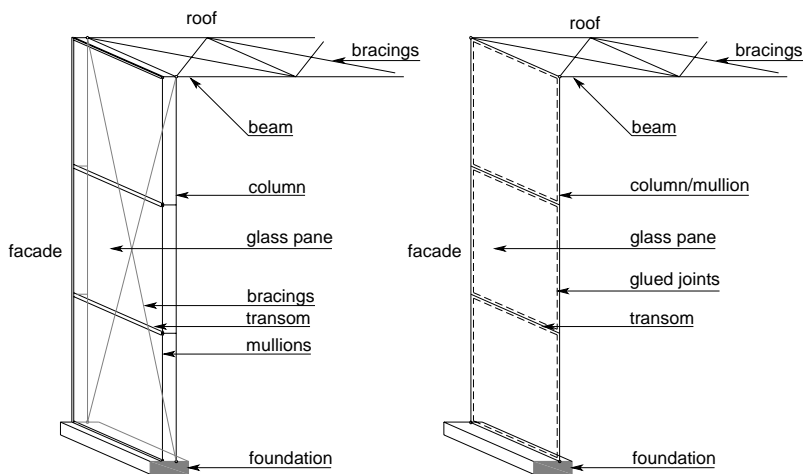


*Figure 1: Separated main bearing structure and façade envelope (left)  
Integrated façade structure with glass panes as shear wall (right)*

Structural requirements of glass façades concern safety and serviceability. Stabilising glass façades have structural advantages such as stiff behaviour, spreading of horizontal loads on the foundation and a slender bearing structure. From an esthetical point of view no annoying bracings have to be applied. This kind of structure can be applied e.g. for entrances, lift shafts, and facades of one or two storey buildings (showrooms).

Regulations [1] of structural application of glass are restricted to glass panes with transversal loads, but no codes are available for in-plane loaded glass panes. The research on in-plane loaded glass is limited [2]. This research concentrates on a steel framework, stabilized with glass panes, bonded to the framework with three different circumferentially glued joints and two types of adhesives. This article concerns the experimental part of the research.

## 2 Glued joint types applied

The system has three different types of glued joints between frame and pane, see Figure 2. Joint type 1 is a glued joint on end and a synthetic material supports the glass pane laterally. The size of the gap between frame and pane depends on tolerances. The gap needs a filling sealant like silicon or polyurethane. The pane is flexibly enclosed. The joint's thickness is a few millimetres.

Joint type 2 is a two-sided circumferentially glued joint. The adhesive epoxy has rigid properties. The joint transfers the in-plane loads and also supports the pane laterally. A gap between glass pane and frame prevents direct glass-metal contact. The thickness of the bond line is very small and has been guaranteed by spacers and adjustable strips.

Joint type 3 is a variant of joint type 2, but it is a one-sided circumferentially glued joint. The joint needs temporary lateral support during curing. An adverse consequence is that the joint is loaded eccentrically.

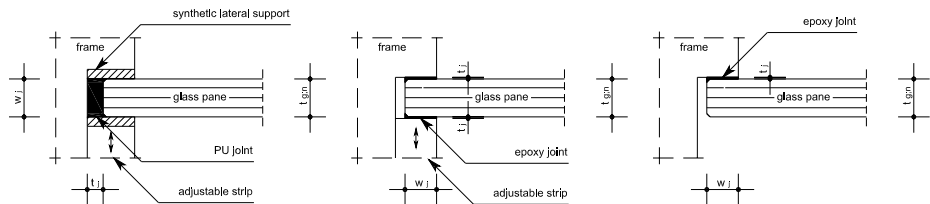


Figure 2: Joint type 1 (left), joint type 2 (centre) and joint type 3 (right)

### 3 Adhesives applied

The joint types have been discussed as well as the choice of adhesive. Two adhesives have been selected for this research. Joint type 1 has polyurethane as joint (SIKAFLEX-252). The sealant like adhesive is a one-component moisture curing glue. Joint types 2 and 3 have epoxy as adhesive (Scotch Weld 9323 B/A), which is a two-component epoxy. The mechanical properties of both adhesives, which are needed, are not given by the specifications of the supplier. The relation between stress and strain has to be known to calculate the joint's stiffness in three orthogonal directions (Figure 3). The stiffness is the quotient of the Young's modulus or shear modulus of the adhesive and the thickness of the joint (Equations 1 and 2).

$$k_1 = \frac{E_a}{t_j} \quad (1)$$

$$k_{2/3} = \frac{G_a}{t_j} \quad (2)$$

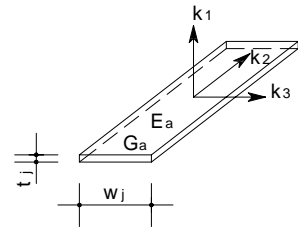


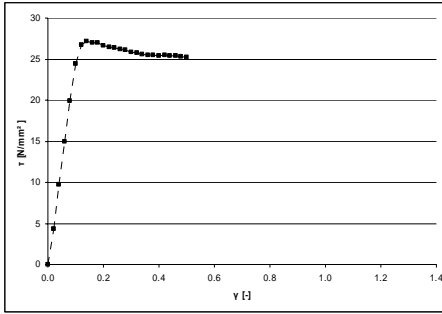
Figure 3: Joint stiffness  $k_1$  to  $k_3$

In which:

- $k_1$  is the normal stiffness in  $\text{N}/\text{mm}^3$
- $k_2/k_3$  is the shear stiffness in  $\text{N}/\text{mm}^3$
- $E_a$  is the Young's modulus of the adhesive in  $\text{N}/\text{mm}^2$
- $G_a$  is the shear modulus of the adhesive in  $\text{N}/\text{mm}^2$
- $t_j$  is the thickness of the glued joint in mm

The shear modulus in Equation 2 has to be determined experimentally. Tensile shear tests are carried out in accordance with DIN 54 451 [3] and ETAG 002 [4]. The results are given in Figure 4 and 5 adopted from [5]. Figure 4 shows the relation between shear stress and shear strain of epoxy under the given conditions. The graph can be divided into two parts. The first part is linear with a constant shear modulus  $G_a = 280 \text{ N}/\text{mm}^2$ . The second part is almost horizontal. The stresses slightly decrease at increasing strains. This is toughened behaviour of the adhesive.

Polyurethane (PU) shows another relation between shear stress and shear strain under the given conditions (Figure 5). The shear strain is larger and the shear stress is clearly smaller than epoxy. This results in a very low shear modulus. Both graphs for epoxy and polyurethane are truncated at a strain of 0.50 and 1.40 respectively, because the specimens tear and rotate. For these values all test specimens fail adhesively.



Storing conditions:

$T = 23^{\circ}\text{C}$

R.H. = 60%

time = 7 days

Geometry bond line:

$t_j = 0.5 \text{ mm}$

$l_j = 5 \text{ mm}$

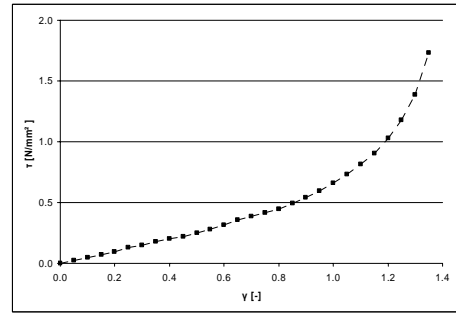
$w_j = 25 \text{ mm}$

Test conditions:

$T = 23^{\circ}\text{C}$

$v = 2.5 \text{ mm/min}$

Figure 4: Shear-strain-relation epoxy



$T = 23^{\circ}\text{C}$

R.H. = 60%

time = 23 days

$t_j = 1.0 \text{ mm}$

$l_j = 18 \text{ mm}$

$w_j = 25 \text{ mm}$

$T = 23^{\circ}\text{C}$

$v = 2.5 \text{ mm/min}$

Figure 5: Shear-strain-relation PU

## 4 Test set-up

The system (Figures 6 and 7) consists of a single glass pane, a steel frame, steel beadwork, three joint types and two types of adhesive. The joint types and mechanical properties of the applied adhesives have been presented in section 2 and 3. The remaining components of the system are described hereafter. The applied shear panel is a single glass pane. The pane applied is annealed float glass with a nominal thickness ( $t_{gm}$ ) of 12 mm. To increase the strength of glass, the edges have facets and have been ground. The steel frame has four rigid beams with width 120 mm and height 59 mm. The beams are connected with a steel bar enclosed by a bearing sleeve to approach a hinge connection at the corners. The beadwork is a replaceable piece of steel and the cross section is joint type dependent (Figure 8). The beadwork is structurally bonded to the primary frame. The system is connected on the testing frame with a pin and a roller. The pin is placed at the same side as the load introduction.

Figure 9 shows the position of the experimental measurements. The load ( $F_h$ ) is introduced by a jack with a deformation rate of 1 mm/min (static load) acting on the centre of the top beam at the right top corner. A load cell measures the magnitude of the load. At the same position the horizontal in-plane displacement is measured (point F). Other in-plane measurements are at the left top corner (point B) and at the left bottom corner (point C). The out-of-plane displacement is measured at point A. At point D and E the relative displacement between frame and glass pane

is measured. Five rosettes measure the strains on the front. Each rosette has three strain gauges (Figure 9), namely a vertical, a horizontal and one at an angle of 45°. These strains are calculated directly to principle stresses. The applied Young's modulus and Poisson's ratio of glass are 70000 N/mm<sup>2</sup> and 0.23 respectively.

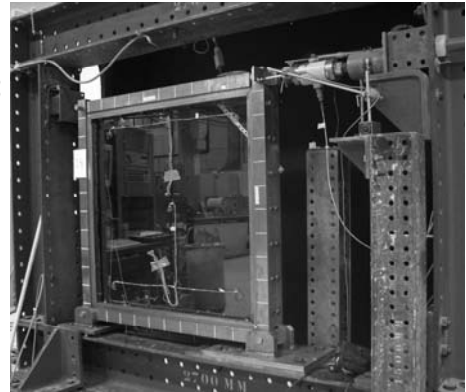
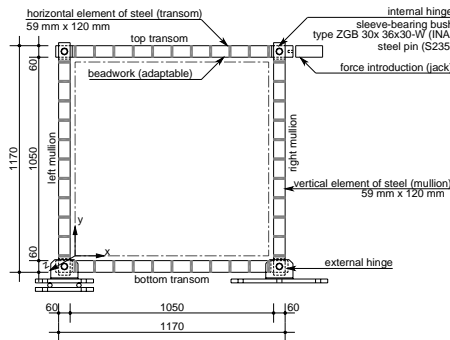


Figure 6: Test set-up (without beadwork)

Figure 7: Picture test set-up (with beadwork)

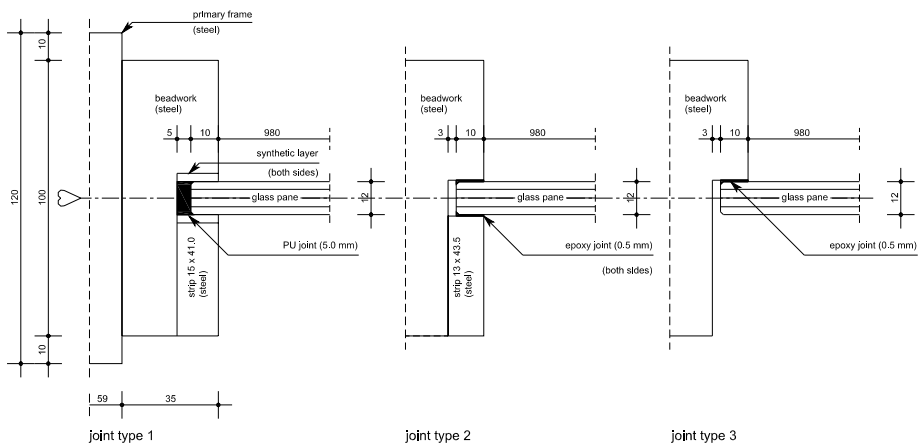


Figure 8: Beadworks belonging to joint type 1 to 3

The tests have been photographically registered with a high speed camera (4000 pictures a second). So, the initial crack and crack propagation through the pane can be followed. The white marking lines on the frame (Figures 6 and 7) are reference lines for the crack analyses.

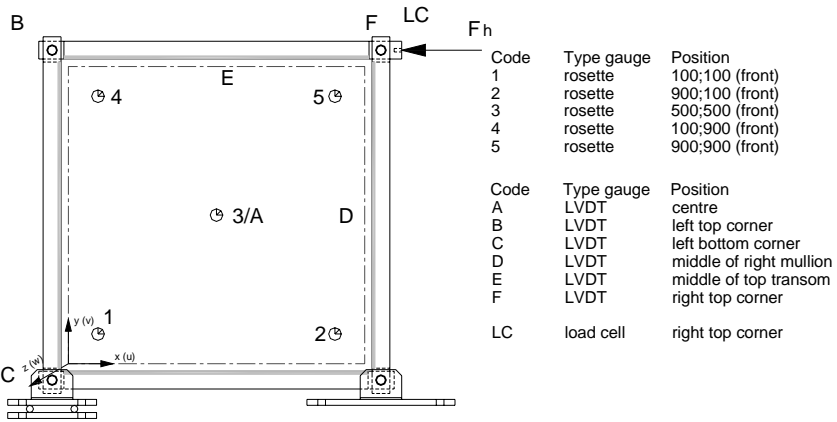


Figure 9: Position of measuring devices

Table 1: Summary test programme

| Joint type                             | 1            | 2              | 3          |
|--|--------------|----------------|------------|
| Valid tests                            | 18, 19, 20   | 1, 2, 3, 4, 17 | 5, 6, 7, 8 |
| Type of adhesive                       | Polyurethane | Epoxy          | Epoxy      |
| Nom. pane size ( $w_g, h_g$ ) [mm]     | 1000         | 1000           | 1000       |
| Nom. glass thickness ( $t_{gn}$ ) [mm] | 12           | 12             | 12         |
| Joint thickness ( $t_j$ ) [mm]         | 5.0          | 0.5            | 0.5        |
| Joint width ( $w_j$ ) [mm]             | 12           | 10             | 10         |
| Curing time [days]                     | 7            | 3              | 3          |

Table 1 gives a summary of the test programme. Systems with joint type 1 are tests 18 to 20, systems of joint type 2 are tests 1 to 4 and 17, and systems with joint type 3 are tests 5 to 8. These tests have valid results. In the following sections the results of each system with joint types 1 to 3 are discussed.

## 5 Flexible joint type on end (joint type 1)

### 5.1 Test results

Figure 10 graphically shows the load-displacement relation at the right top corner ( $u_r$ ). The diagram has two parts. The first part shows a linear relation with large displacements and small



loads. No cracks occur during the first part. The second part shows a rapid increase of load accompanied by cracking.

Tables 2a and 2b give an overview of the measuring results at the intersection of two curves and maximum load respectively. The in-plane displacements of the left top corner ( $u_B$ ) are smaller than the displacements at load introduction ( $u_F$ ). The left bottom corner has small displacements ( $u_C$ ). The relative displacements at point D and E measure the resultant of the horizontal and vertical displacements. Point D horizontally displaces from the right mullion and vertically displaces to the top. The top transom horizontally displaces more than the pane at point E. The vertical displacement is from the top transom. The out-of-plane displacements ( $w_A$ ) are small and to the rear side.

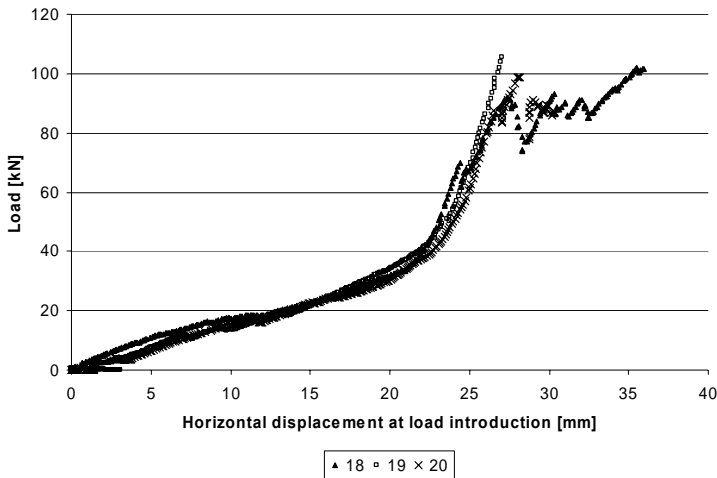


Figure 10: Load-displacement diagram of systems with joint type 1 (polyurethane)

Figure 11 schematically shows the simplified crack patterns. The glass pane shifts and rotates within the frame in the given direction. The firstly perceived crack is shattering a piece of glass at the right top corner (only for test 20 at the left bottom corner). Then the pane gradually cracks further at the right top corner and pieces of broken glass fall down. By cracking at this corner, the load is introduced by the right mullion to the glass pane. At increasing load the pane further rotates in the frame. This results in peeling off the glued joint from the pane at tensile stresses and pushing away the bond line at compression stresses (glass-metal contact).

Table 2a: Overview measuring results of test series with joint type 1 at intersection of two curves

| Test             | 18                   | 19                   | 20                   | Average | Standard deviation |
|------------------|----------------------|----------------------|----------------------|---------|--------------------|
| $F_h$ [kN]       | 36.87                | 38.99                | 39.40                | 38.42   | 1.36               |
| $u_F$ [mm]       | 21.58                | 21.43                | 22.52                | 21.84   | 0.59               |
| $w_A$ [mm]       | 0.38 <sup>(1)</sup>  | 0.25 <sup>(1)</sup>  | 0.42 <sup>(1)</sup>  | 0.35    | 0.09               |
| $u_B$ [mm]       | 19.94                | 20.63                | 18.97                | 19.85   | 0.83               |
| $u_C$ [mm]       | 0.11                 | 0.19                 | 0.18                 | 0.16    | 0.04               |
| $u_{D,rel}$ [mm] | 5.54 <sup>(2)</sup>  | 7.18 <sup>(2)</sup>  | 5.76 <sup>(2)</sup>  | 6.16    | 0.89               |
| $u_{E,rel}$ [mm] | -6.12 <sup>(3)</sup> | -6.57 <sup>(3)</sup> | -6.01 <sup>(3)</sup> | -6.23   | 0.30               |

Table 2b: Overview measuring results of test series with joint type 1 at maximum load

| Test       | 18                  | 19                  | 20                  | Average | Standard deviation |
|------------|---------------------|---------------------|---------------------|---------|--------------------|
| $F_h$ [kN] | 91.54               | 105.50              | 98.75               | 98.60   | 6.98               |
| $u_F$ [mm] | 27.30               | 27.01               | 28.18               | 27.50   | 0.61               |
| $w_A$ [mm] | 1.24 <sup>(1)</sup> | 1.32 <sup>(1)</sup> | 1.28 <sup>(1)</sup> | 1.28    | 0.04               |
| $u_B$ [mm] | 25.31               | 26.27               | 24.63               | 25.40   | 0.82               |
| $u_C$ [mm] | 0.57                | 0.63                | 0.61                | 0.60    | 0.03               |

<sup>(1)</sup> Measured deformation to the rear side

<sup>(2)</sup> Pane moves more than right mullion

<sup>(3)</sup> Pane moves less than top transom

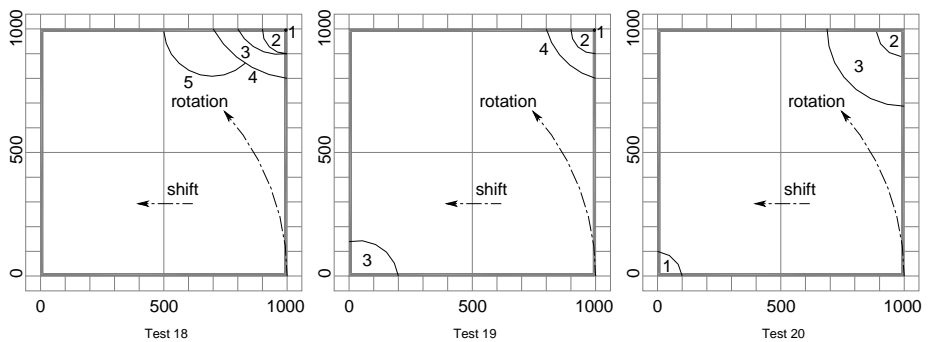
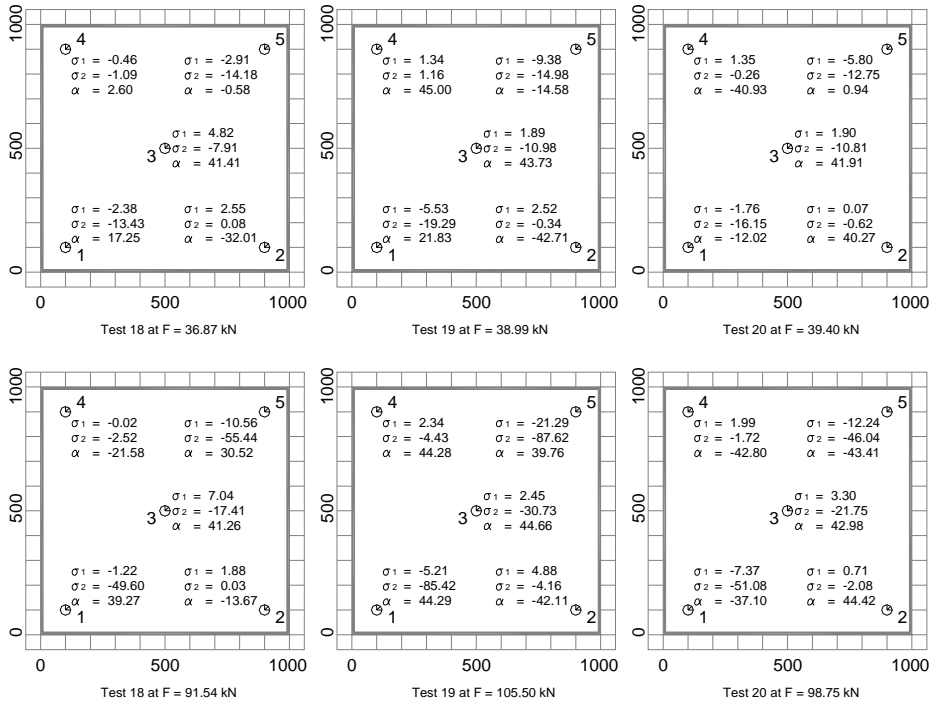


Figure 11: Simplified crack patterns of test series with joint type 1

Figure 12 shows the principle stresses and their directions of points 1 to 5 at loads mentioned in Tables 2a and 2b. The principle stresses at points 2 and 4 are very small compared to points 1, 3 and 5. The minimum principle stresses at points 1 and 5 are larger than at point 3.



$\sigma_1$  is the maximum principle stress calculated from measured strains

$\sigma_2$  is the minimum principle stress calculated from measured strains

$\alpha$  is the angle between horizontal and maximum principle stress (positive is clockwise)

Figure 12: Principle stresses (on front) and their directions of test series with joint type 1 at intersection of two curves (top) and maximum load (bottom)

## 5.2 Explanation of test results

The large displacement of the first part of the load-displacement diagram has been caused by shifting and rotating of the glass pane within the steel frame. The steel frame deforms from a square to a rhomb. The diagonal of the pane from left bottom corner to right top corner acts as compression strut. The joint between steel frame and glass pane becomes smaller at increasing load. The load has been spread and therefore no cracks occur.

At the intersection of two curves the diagonal of the rhomb is the diagonal of the glass pane. The thickness of the joint has been pushed in and this is the start of the second part of the load-

displacement diagram. The same diagonal of the pane also acts as compression strut. The load introduction leads to larger stresses at both ends of the compression diagonal and leads to cracking.

This system can be simplified as a system with three structural components, namely the right mullion, the bottom transom and the compressed diagonal of the glass pane with an effective width. The out-of-plane displacements are small and the structure can be considered as geometrically linear.

### 5.3 Analytical analysis

Figure 13 shows the undisplaced system (left) and the displaced system (right). The assumption is that the diagonal ( $d_g$ ) of the glass pane and the steel frame ( $l_{gr}$ ) are undeformed. The steel frame displaces from a square to a rhomb. The glass pane shifts and rotates within the rhomb of the steel frame. This displacement mechanism stops when the diagonal of the pane is the diagonal of the rhomb. The horizontal displacement at the top transom ( $u_F, u_B$ ) is represented by Equation 3. The displaced situation at points D and E (Figure 13 right) shows a displacement difference between frame and pane. These displacements are the resultant of the horizontal and the vertical displacement. This is the relative displacement ( $u_{D,rel}, u_{E,rel}$ ) and can be calculated with Equation 4.

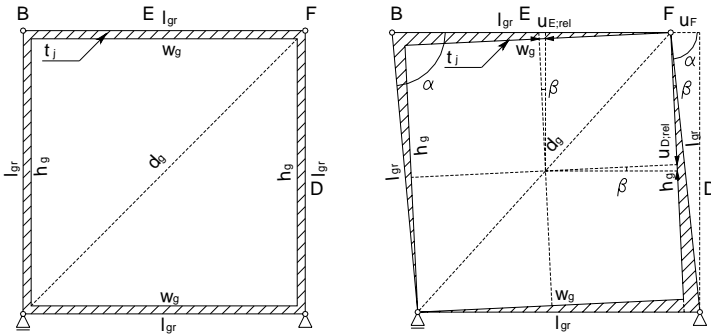


Figure 13: Not displaced frame (left), shifted and rotated glass pane within the rhomb of the frame (right)

$$u_F = u_B = l_{gr} - \frac{d_g^2}{2l_{gr}} \quad (3)$$

$$u_{D,rel} = u_{E,rel} = \sqrt{\left(\frac{1}{2}(l_{gr} - h_g)\right)^2 + \left(\left(\frac{2l_{gr}h_g - d_g^2}{4l_{gr}^2}\right) \cdot h_g\right)^2} \quad (4)$$

In which:

- $u_{B/F}$  is the horizontal displacement of the top beam at point B and F respectively in mm
- $d_g$  is the length of the diagonal of the glass pane in mm
- $l_{gr}$  is the length of the groove in mm
- $u_{D/E,rel}$  is the relative displacement between pane and frame at point D and E respectively in mm
- $h_g$  is the height of the glass pane in mm

The displacement of points B, F, D and E can be calculated with Equations 3 and 4 respectively. The diagonal length of the pane ( $d_g = 1416$  mm), the height of the pane ( $h_g = 1001$  mm) and the groove length ( $l_{gr} = 1011$  mm) are measured with 1 mm precision. These values substituted in Equations 3 and 4 gives for the horizontal displacement  $u_B = u_F = 19.38$  mm and for the relative displacement  $u_{D,rel} = u_{E,rel} = 6.82$  mm. Table 2a shows the measured values of these points. The calculated values of points B and F and D and E slightly deviate from the measured values.

The load transfer is from the right top corner to the left bottom corner (compression strut). The principle stresses at point 1 and 5 depend on the edge conditions, but the stress at point 3 can be calculated with the 'one third rule' of Holmes [6]. The effective width of the compression strut is one-third of the diagonal length. The equation is:

$$\sigma_{g,N} = -\frac{3\sqrt{2} F_{h(max)}}{t_{g,ave} d_g} \quad (5)$$

In which:

- $\sigma_{g,N}$  is normal stress in the compressed diagonal in N/mm<sup>2</sup>
- $F_{h(max)}$  is the (maximum) horizontal load acting at the right top corner in N
- $t_{g,ave}$  is the average thickness of the glass pane in mm
- $d_g$  is the length of diagonal of the compressed glass strut in mm

Table 3: Normal stress in compressed diagonal based on 'one third rule' at point 3

| Test   | 18     | 19     | 20     | 18     | 19     | 20     |
|--|--------|--------|--------|--------|--------|--------|
| $F_{h(max)}$ [kN]                                      | 36.87  | 38.99  | 39.40  | 91.54  | 105.50 | 98.75  |
| $t_{g,ave}$ [mm]                                       | 12.026 | 12.041 | 12.026 | 12.026 | 12.041 | 12.026 |
| $\sigma_{g,N}$ [N/mm <sup>2</sup> ]                    | -9.19  | -9.70  | -9.82  | -22.81 | -26.25 | -24.60 |
| $\frac{\sigma_2 - \sigma_{g,N}}{\sigma_2} \cdot 100\%$ | -16.18 | 11.67  | 9.16   | -31.02 | 17.07  | -13.10 |

Table 3 gives the results of the calculated normal stress ( $\sigma_{g;N}$ ) and compares these stresses with the minimum principle stress ( $\sigma_2$ ) at point 3 (Figure 12). The calculated normal stresses vary between -16.18% and 17.07%. Test 18 gives the largest deviation. Equation 5 is based on a simple rule of thumb and has to be improved with finite element simulations.

## 6 Two-sided rigid joint (joint type 2)

### 6.1 Test results

The second test series have circumferentially two-sided glued joints (see Figure 2). Figure 14 shows the relation between load and horizontal displacement at the right top corner. The load-displacement diagram is a gradually declining curve with some discontinuities caused by cracking of the glass pane.

Tables 4a and 4b give an overview of the measuring results at a load of about 46.00 kN and at maximum load. At about 46.00 kN all panes are uncracked and are comparable to each other. The maximum load shows a large deviation for the five tests. The in-plane displacements at left top corner ( $u_B$ ) are smaller than the in-plane displacements at right top corner ( $u_F$ ). The left bottom corner slightly displaces ( $u_C$ ). The out-of-plane displacements ( $w_A$ ) are small except for test 1 at maximum load. These displacements are to the rear side. The relative displacements ( $u_{D,rel}$  and  $u_{E,rel}$ ) are very small for both loads.

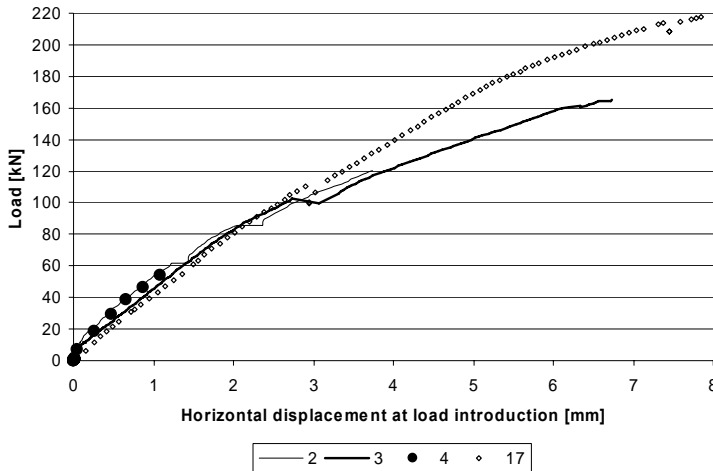


Figure 14: Load-displacement diagram of systems with joint type 2 (epoxy)

Table 4a: Overview measuring results of test series with joint type 2 at about 46.00 kN

| Test       | 1     | 2                   | 3                   | 4                   | 17                  | Average <sup>(2)</sup> | Standard deviation |
|------------|-------|---------------------|---------------------|---------------------|---------------------|------------------------|--------------------|
| $F_h$ [kN] | 45.15 | 45.92               | 44.90               | 46.35               | 46.86               | 46.00                  | 0.83               |
| $u_F$ [mm] | --    | 0.95                | 0.98                | 0.92                | 1.14                | 1.00                   | 0.10               |
| $w_A$ [mm] | 0.50  | 0.54 <sup>(1)</sup> | 0.26 <sup>(1)</sup> | 0.45 <sup>(1)</sup> | 0.45 <sup>(1)</sup> | 0.43                   | 0.12               |
| $u_B$ [mm] | --    | 0.82                | 0.50                | 0.87                | 0.62                | 0.70                   | 0.17               |
| $u_C$ [mm] | --    | 0.25                | 0.12                | 0.10                | 0.02                | 0.12                   | 0.10               |

Table 4b: Overview measuring results of test series with joint type 2 at maximum load

| Test       | 1                     | 2                     | 3                   | 4                    | 17                  |
|------------|-----------------------|-----------------------|---------------------|----------------------|---------------------|
| $F_h$ [kN] | 117.27 <sup>(3)</sup> | 120.47 <sup>(3)</sup> | 165.05              | 96.14 <sup>(4)</sup> | 218.02              |
| $u_F$ [mm] | --                    | 4.23                  | 6.73                | --                   | 7.85                |
| $w_A$ [mm] | 2.52                  | 1.13 <sup>(1)</sup>   | 0.55 <sup>(1)</sup> | --                   | 0.96 <sup>(1)</sup> |
| $u_B$ [mm] | --                    | 3.74                  | 5.80                | --                   | 7.25                |
| $u_C$ [mm] | --                    | 1.13                  | 0.98                | --                   | 0.92                |

<sup>(1)</sup> Displacement to rear side

<sup>(2)</sup> Excluding test 1

<sup>(3)</sup> Test has been stopped arbitrary at this load

<sup>(4)</sup> The maximum value is 96.14 kN, but after 53.78 kN all displacement measurements are incorrect

Figure 15 shows the simplified crack patterns. The first crack of test 1 initiates at the left bottom corner at load 45.39 kN. This small crack quickly propagates to the right top corner and splits the pane into two triangular pieces of glass (2). The system is still stable in this situation.

The first cracks of test 2 occur at the right bottom corner at load 45.93 kN and has a fan-like crack pattern. The second and third crack occurs at load 63.37 kN and at load 85.91 kN respectively at the same corner. The fractures are parallel to the compression diagonal. The final cracks (4) starts at the left bottom corner at load 120.47 kN. These cracks are also parallel to the compression diagonal.

The first crack of test 3 occurs at the right bottom corner at load 102.44 kN and has also a fan-like crack pattern. Just before the final cracks, a crack occurs parallel to the compression diagonal at the right bottom corner (2). The final cracks (3) start at the left transom and propagate to the right top corner at load 164.32 kN. A triangular piece of glass pane bounces out between the left bottom, right bottom and right top corner (dotted area).

The first crack of test 4 initiates at the left bottom corner and rapidly propagates through the pane to the right top corner at load 53.78 kN. This crack stops with a fan-like pattern. The pane is separated into two triangular pieces of glass. The second crack occurs at the right bottom corner at load 80.49 kN and has a fan-like pattern. The third crack is parallel to the first crack at load 89.46 kN. Finally, the diagonal from the left bottom corner to the right top corner (dotted area) bounces out at load 96.14 kN.

The first cracks of test 17 occur at load 110.44 kN and the crack pattern is the same as at test 2 and 3. The second series of cracks start from the left top corner at load 210.12 kN and quickly followed by the third series of cracks at load 213.69 kN. These cracks gradually move parallel to the compression diagonal. The entire pane (dotted area) bounces out at 218.02 kN initiated at the left bottom corner.

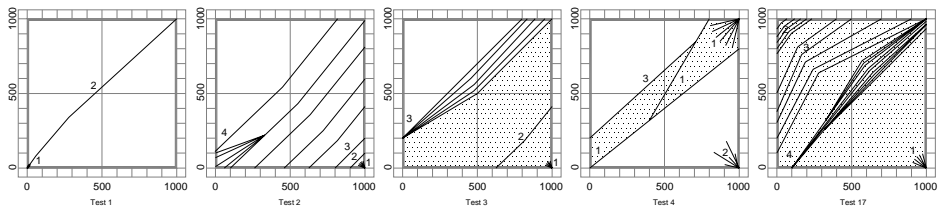


Figure 15: Simplified crack patterns of test series with joint type 2

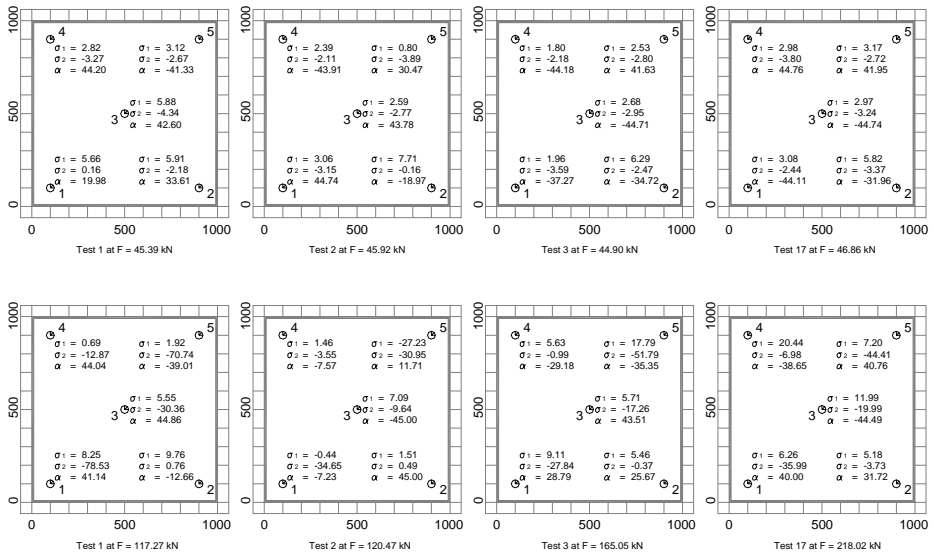
Figure 16 shows the principle stresses and their directions. The values of the principle stresses are small for each point about load 46.00 kN (Figure 16 top). The minimum principle stresses are compression stresses and the maximum principle stresses are tensile stresses, except for point 1 of test 1. The values of the minimum principle stresses at maximum load (Figure 16 bottom) are large at points 1, 3 and 5.

## 6.2 Explanation of test results

The load-displacement diagram of each test has the same path, but the cracks interrupt the image. The stiffness gradually declines with increasing load. The horizontal displacement of the top transom depends on shear deformation of the pane and glued joints. These displacements are small that the contribution of the margins of the system can play a role. The relative deformations of the epoxy joint are very small at points D and E. So, the pane can not deform freely within the deformed frame. The out-of-plane displacements are small and also behave



geometrically linear. Test 1 shows a larger out-of-plane displacement, because point A has moved to the front after dividing the pane into two triangular pieces of glass.



$\sigma_1$  is the maximum principle stress calculated from measured strains  
 $\sigma_2$  is the minimum principle stress calculated from measured strains  
 $\alpha$  is the angle between horizontal and maximum principle stress (positive is clockwise)

Figure 16: Principles stresses (on front) and their directions of test series with joint type 2

The fan-like cracks at the right bottom corner are the result of tensile stresses. Three tensile stresses converge on this corner, namely from the right mullion, the bottom transom and the tensile diagonal of the pane. The pane locally cracks and has very small effect on the system. The other cracks are parallel to the compression diagonals, because tensile diagonals act perpendicular to the compression diagonals.

All tests show a post-cracking behaviour. Several cracks have to occur before cracking of the entire pane. The systems of test 1 to 4 are still able to resist load after the test has stopped, because of the remaining triangular pieces of glass at the left top corner and/or right bottom corner.

The principle stresses at about load 46.00 kN are distributed uniformly and their directions are approximately 45°. This image belongs to a shear panel with uniform shear load around the edges. The principle stress at maximum load clearly shows large compression stresses in the

compression diagonal, but the pane also transfers load through the entire pane. So, the pane still acts as a shear panel with other shear load distribution around the edges.

### 6.3 Analytical analysis

The glass pane is loaded by uniform distributed shear load around the perimeter. The shear stresses in the pane are the quotient of horizontal load and the product of pane thickness and joint length. These shear stresses are transformed into principle stresses. Equation 6 calculates the average maximum and minimum principle stresses of the pane and their directions are 45°. The average shear stresses in the joint are given in Equation 7. The equation is comparable to Equation 6, but the pane thickness is replaced by two times the joint thickness. Equation 8 gives average deformation of the joint and based on the quotient shear stress and shear stiffness (Equation 2) of the joint.

$$\sigma_{1/2;cal} = \pm \frac{F_h}{t_{g,ave} l_j} \quad (6)$$

$$\tau_{j,ave} = \frac{F_h}{2w_j l_j} \quad (7)$$

$$u_{j,ave} = \frac{\tau_{j,ave}}{k_2} \quad (8)$$

In which:

|                  |   |
|------------------|---|
| $F_h$            | is the horizontal load in N   |
| $\sigma_{1;cal}$ | is calculated maximum principle stress in N/mm <sup>2</sup>         |
| $\sigma_{2;cal}$ | is calculated minimum principle stress in N/mm <sup>2</sup>         |
| $t_{g,ave}$      | is the average thickness of the glass pane in mm                    |
| $\tau_{j,ave}$   | is the average shear stress of the joint in N/mm <sup>2</sup>       |
| $u_{j,ave}$      | is the average deformation of the joint in mm                       |
| $w_j$            | is the width of the joint in mm                                     |
| $l_j$            | is the length of the joint in mm                                    |
| $t_j$            | is the thickness of the joint in mm                                 |
| $k_2$            | is the shear stiffness of the joint in N/mm <sup>3</sup> (Figure 3) |

Table 5 gives the results of Equations 6 to 8. The calculated average maximum and minimum principle stresses are larger than the measured values, except for the maximum principle stress at the right bottom corner (point 2) for all tests and for test 1 at points 1 and 3. The shear stress

and deformation of the joint is very small and is within the linear relation between the shear stress and strain (Figure 4).

Equations 6 to 8 also apply at larger loads. Nevertheless, the compression stresses at points 1, 3 and 5 are significantly larger than at points 2 and 4. These large compression stresses are not the consequence of glass steel contact. Table 6 gives the results of Equations 6 to 8 for maximum load. Test 1 is not considered in this table, because the pane is divided into two pieces of glass at about 46.00 kN and gives another stress distribution. The average minimum principle stresses are smaller than measured (Figure 16), except for test 2. The shear stress and deformation of the joint is larger than around 46.00 kN and is also within the linear relation between the shear stress and strain (Figure 4).

Table 5: Calculated stresses in pane and joint at points 1 to 5 at about 46 kN

| Test                                    | 1      | 2      | 3      | 17     |
|---|--------|--------|--------|--------|
| $F_h$ [kN]                              | 45.39  | 45.92  | 44.90  | 46.86  |
| $t_{g,ave}$ [mm]                        | 11.945 | 11.900 | 12.035 | 12.045 |
| $\sigma_{1/2,cal}$ [N/mm <sup>2</sup> ] | 3.84   | 3.90   | 3.77   | 3.93   |
| $\tau_{j,ave}$ [N/mm <sup>2</sup> ]     | 2.29   | 2.32   | 2.27   | 2.37   |
| $u_{j,ave}$ [mm]                        | 0.0040 | 0.0042 | 0.0040 | 0.0042 |

$w_j = 10$  mm;  $l_j = 990$  mm;  $t_j = 0.50$  mm;  $k_2 = 560$  N/mm<sup>3</sup> (Equation 2)

Table 6: Minimum principle stress ( $\sigma_2$ ) at point 3 and shear stress ( $\tau_{j,ave}$ ) and deformation ( $u_{j,ave}$ ) of joint at maximum load

| Test                                | 2      | 3      | 17     |
|-------------------------------------|--------|--------|--------|
| $F_h$ [kN]                          | 120.47 | 165.05 | 218.02 |
| $t_{g,ave}$ [mm]                    | 11.900 | 12.035 | 12.045 |
| $\sigma_2$ [N/mm <sup>2</sup> ]     | -10.23 | -13.85 | -18.28 |
| $\tau_{j,ave}$ [N/mm <sup>2</sup> ] | 6.08   | 8.34   | 11.01  |
| $u_{j,ave}$ [mm]                    | 0.0073 | 0.0100 | 0.0131 |

$w_j = 10$  mm;  $l_j = 990$  mm;  $d_g = 1416$  mm;  $k_2 = 560$  N/mm<sup>3</sup> (Equation 2)

Equations 6 to 8 have to be improved. The shift between load introduction and glass pane-joint is not involved and leads to shear stresses perpendicular to the joint length and is also loaded with normal stresses (lateral support). At larger loads, the compression strut transfers more load

than points 2 and 4. These equations are based on simple theory of mechanics and have to be refined by finite element method to investigate these influences on the stress distribution of the pane.

## 7 One-sided rigid joint type (joint type 3)

### 7.1 Test results

Figure 17 graphically shows the load-displacement relation at the right top corner. The displacement is small and the maximum load is also the collapse load. During increasing of the load the pane regularly cracks.

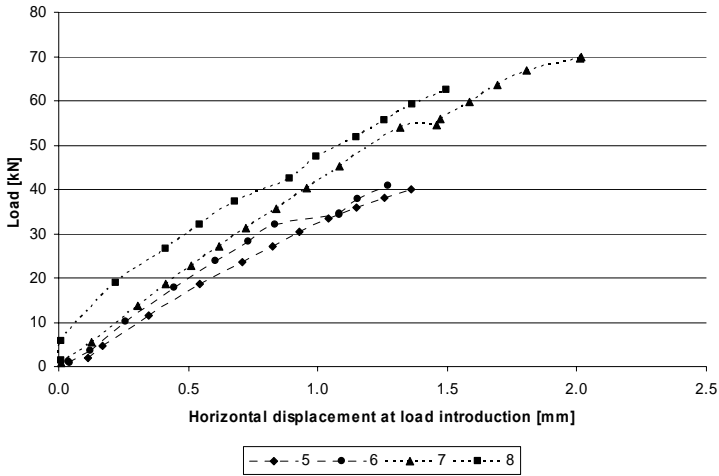


Figure 17: Load-displacement diagram of system of test series with joint type 3 (epoxy)

Table 7: Overview measuring results of test series with joint type 3

| Test       | 5                   | 6                   | 7                   | 8                   | Average | Standard deviation |
|------------|---------------------|---------------------|---------------------|---------------------|---------|--------------------|
| $F_h$ [kN] | 38.62               | 40.87               | 69.94               | 62.53               | 52.99   | 15.62              |
| $u_F$ [mm] | 2.47                | 1.27                | 2.02                | 1.41                | 1.79    | 0.56               |
| $w_A$ [mm] | 1.48 <sup>(2)</sup> | 0.27 <sup>(1)</sup> | 0.83 <sup>(1)</sup> | 0.71 <sup>(1)</sup> | 0.82    | 0.50               |
| $u_B$ [mm] | 2.41                | 1.14                | 1.93                | 1.50                | 1.75    | 0.55               |
| $u_C$ [mm] | 0.12                | 0.18                | 0.27                | 0.29                | 0.22    | 0.08               |

<sup>(1)</sup> Measured displacement to the rear side

<sup>(2)</sup> Measured displacement to the front side

Table 7 gives an overview of measured loads and displacements. Tests 5 and 6 have lower maximum loads than tests 7 and 8. The in-plane displacement at the right top corner ( $u_r$ ) significantly deviates with accompanying load. The in-plane displacement at the left top corner ( $u_l$ ) has slightly smaller displacements than measured at the right top corner, except for test 8. The out-of-plane displacement of the centre ( $w_A$ ) is small and deforms to the rear side, except for test 5. The left bottom corner has small in-plane displacements ( $u_c$ ). The relative displacement between glass pane and frame at points D and E are very small and can be considered as zero.

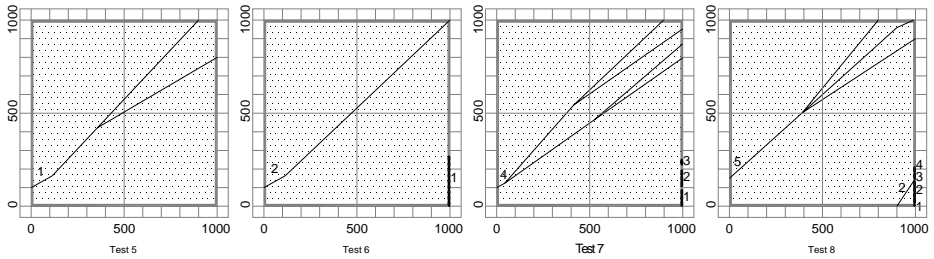


Figure 18: Simplified crack patterns of test series with joint type 3

Figure 18 shows the simplified crack patterns. Test 5 starts cracking at the bottom of the left mullion at load 38.62 kN. This crack quickly propagates to the right top corner. The first crack of tests 6, 7 and 8 is along the right transom on the glued joint at load 31.99 kN, 53,98 kN and 37.25 kN respectively. Test 7 and 8 cracks further on the glued joint. The final crack of test 6, 7 and 8 starts at the bottom of the left mullion at load 40.87 kN, 69.94 kN and 62.53 kN respectively. All panes start breaking at approximately 100 mm above the left bottom corner at maximum load.

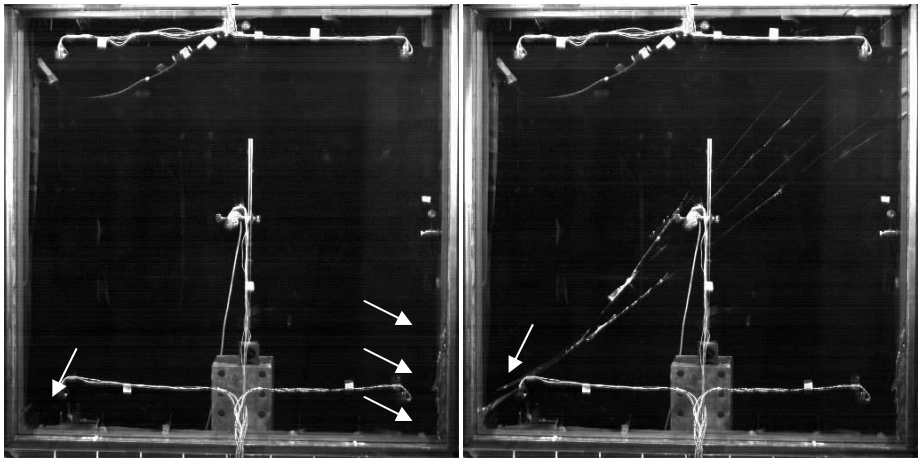
Figure 19 (left) shows the situation just before the final crack of test 7 recorded by the high speed camera. The location, where the final crack initiates, shows a small sparkle. Figure 19 (right) shows the crack propagation 0.0225 seconds after initiating the crack.

Figure 20 shows the principle stresses and their directions. The minimum principle stresses are compression stresses and the maximum principle stresses are tensile stresses. The stresses are small at each point except at points 1 of test 5 and 6.

## 7.2 Explanation of test results

The load-displacement diagram of each test has the same path, but the cracks interrupt the image. The relation is linear which tends to decline with increasing load. The horizontal displacement of the top transom depends on shear deformation of the pane and glued joints.

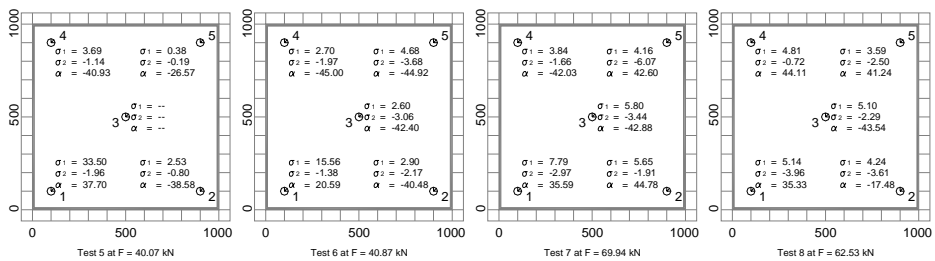
These displacements are very small and the contribution of the margins of the system also plays a role. The relative deformations of the epoxy joint are very small at points D and E. So, the pane can not deform freely within the deformed frame. The out-of-plane displacements are small and also behave geometrically linear.



Left: Initiating crack 4, cracked zone along right transom.

Right: 90/4000 seconds after initiating crack 4.

Figure 19: High speed pictures of test 7



$\sigma_1$  is the maximum principle stress calculated from measured strains

$\sigma_2$  is the minimum principle stress calculated from measured strains

$\alpha$  is the angle between horizontal and maximum principle stress (positive is clockwise)

Figure 20: Principle stress (on front) and directions of test series with joint type 3

The cracks along the right transom on the glued joint are the result of tensile stresses from the right mullion, bottom transom, the tensile diagonal of the pane and by eccentric connection. The pane locally cracks and has very small effect on the system. The final crack starts at the bottom of the left mullion and is parallel to the compression diagonal.

All tests show a post-cracking behaviour, except for test 5. Tests 6 to 8 have several cracks before collapsing of the pane. After collapsing the pane, the system has no remaining capacity. The eccentricity negatively influences the behaviour of the system.

The principle stresses at maximum load are distributed uniformly and their directions are approximately 45°. This image belongs to a shear panel with uniform shear load around the edges.

### 7.3 Analytical analysis

The glass pane is loaded by shear load around the perimeter. The shear stresses in the pane are the quotient of horizontal load and the product of pane thickness and joint length. These shear stresses are transformed into principle stresses. Equation 6 calculates the average maximum and minimum principle stresses of the pane and their direction is 45°. The average shear stresses in the joint are given in Equation 9. The equation is comparable to equation 6, but the thickness of the pane is replaced by the joint thickness. Equation 8 gives average deformation of the joint and based on the quotient shear stress and shear stiffness (Equation 2) of the joint.

$$\tau_{j,ave} = \frac{F_h, \max}{w_j l_j} \quad (9)$$

Table 8 shows the results of Equations 6, 8 and 9. The average calculated principle stresses ( $\sigma_{1,2}$ ) are larger than measured (Figure 21), except for maximum principle stress at the left bottom corner (point 1) of tests 5 to 7 and the right top corner (point 5) of test 6. The average shear stresses of the joint ( $\tau_{j,ave}$ ) are small and are in the linear relation between shear stress and strain (Figure 4). Therefore, the accompanying average joint deformations are also small.

Table 8: Calculated principle stresses ( $\sigma_1$  and  $\sigma_2$ ) and joint deformation of point 1 to 5

| Test                                | 5      | 6      | 7      | 8      |
|-------------------------------------|--------|--------|--------|--------|
| $F_h$ [kN]                          | 40.07  | 40.87  | 69.94  | 62.53  |
| $t_{g,ave}$ [mm]                    | 12.025 | 12.035 | 12.045 | 12.005 |
| $\sigma_{1/2}$ [N/mm <sup>2</sup> ] | 3.37   | 3.43   | 5.87   | 5.26   |
| $\tau_{j,ave}$ [N/mm <sup>2</sup> ] | 4.05   | 4.13   | 7.06   | 6.32   |
| $u_{j,ave}$ [mm]                    | 0.0072 | 0.0074 | 0.0126 | 0.0112 |

$w_j = 10$  mm;  $l_j = 990$  mm;  $t_j = 0.50$  mm;  $k_2 = 560$  N/mm<sup>3</sup> (Equation 2)

Equation 6 has to be improved, because the eccentrically placed joint and eccentric load introduction are not involved and play a considerable role to predict the maximum principle

stress. The Equations 8 and 9 also have to be improved, because the joint is also loaded with normal stresses (lateral support and eccentricity) and shear stresses along the joint width (eccentric load introduction). These equations are based on simple theory of mechanics. Finite elements simulations will be used to investigate these influences on the stress distribution in the pane.

## 8 Evaluation of test results

Systems with joint type 1 clearly have the smallest system stiffness in comparison to systems with joint types 2 and 3. The horizontal displacement of the first part is caused by shifting and rotating of the glass pane within the system. At larger loads these systems show a larger stiffness (second part), because the shifted and rotated glass pane is fixed in the displaced frame. Systems with joint types 2 and 3 have large system stiffness. The contribution of the horizontal displacement is the sum of margins of the system, deformation of joint and glass pane.

Systems with joint type 1 transfer the load through a compression strut in the pane. The stress distribution is uniform for systems with joint type 3 and for joint type 2 at lower loads. At larger load, systems with joint type 2 mainly transfer the load through a compression strut in the pane.

Systems with joint type 1 show no cracks at small loads, but cracks occur at the corners of the compression strut at larger loads. Systems with joint types 2 and 3 regularly show cracks during increasing of the load. The first cracks for both systems occur at the right bottom corner. This corner is subjected to three tensile forces from the right mullion, the bottom transom and tensile diagonal of the pane. System with joint type 3 has an additional tensile stress from bending by eccentrically glued joint. The entire pane cracks from the left bottom corner to the right top corner. The cracks are parallel to the compression diagonal and perpendicular to the tensile diagonal.

The average maximum load of systems with joint type 1 is 98.00 kN. The systems are able to resist larger loads accompanying with larger displacement. The maximum load of systems with joint type 2 varies between 96.14 kN and 218.02 kN. The maximum load is for both systems not the collapse load, except for test 17 with 218.02 kN. The maximum load of systems with joint type 3 varies between 38.62 kN and 69.94 kN and is also the collapsing load. The pane is unfavourably loaded by the eccentrically placed joint.



The in-plane loaded glass pane is less sensitive for out-of-plane displacements for all systems, because the ratio thickness ( $t_{gn} = 12$  mm) width ( $w_g = 1000$  mm) is very small.

Finally, all tests have a good 'warning mechanism', because annealed float glass is applied. Annealed float glass does not fully collapse after the first crack occurs and even not by further cracking.

## 9 Conclusions

Three shear wall systems with different joints are tested. The stress distribution and displacement of the system are analyzed. The following conclusions can be drawn with regard to safety and serviceability.

Systems with joint type 1 have large horizontal displacement, because the pane is flexibly enclosed. Nevertheless, the system is able to resist an average load of 38.42 kN without cracking. If all panes in a façade are connected with this flexible joint, the horizontal displacement of the shear wall is acceptable. The vertically placed glass panes have to transfer the horizontal load, but the deformation increases with the height (serial connected system). The horizontally placed glass panes distribute the horizontal load on each vertically placed glass panes (parallel connected system). The load is transferred by a 'compression' strut. The system can even resist larger loads accompanying by cracking and larger horizontal deformations. The cracked pane is still able to transfer load. The system has a good 'warning mechanism' for failure.

Systems with joint type 2 exhibit stiffer behaviour. Therefore, a few bays of glass panes have to be structurally bonded for acceptable horizontal displacement of the façade. The stress distribution at small loads ( $F_{h,ave} = 46.00$  kN) belongs to a shear wall. The cracked pane can resist larger loads and the horizontal displacement remains small. The load transfer is more concentrated in the 'compression' strut. The system has a good 'warning mechanism' for failure.

Systems with joint type 3 are comparable to systems with joint type 2. In the design of a stabilising façade, a few bays of structurally bonded glass panes with joint type 3 give acceptable horizontal displacement. The stress distribution belongs to a shear wall. The cracked pane can resist larger load and the system has a good 'warning mechanism'. But if the final crack occurs, the pane is eliminated in the load transfer. This is attributed to the eccentrically placed joint. Therefore, the horizontal load is much smaller than the load for systems with joint type 2.

## 10 Future research

The experimental research will be continued to determine the modulus under tensile and compression load. These values are necessary to calculate the normal stiffness ( $k_i$ ) of the joint. The following step is a numerical research including a parameter study to investigate the location of the maximum principle stress (failure criteria for glass). The finite element programme DIANA will be used, because this programme has a tool to model the joint's stiffness including the non-linear behaviour. The numerical results will be validated using the experimental data. Finally, a design rule has to be developed for the design of a steel frame, stabilized by a circumferentially glued glass pane.

## References

- [1] NEN 2608-2 (2004), Vlakglas voor gebouwen – Deel 2: Niet-verticaal geplaatst glas – Weerstand tegen windbelasting, sneeuw, eigengewicht – Eisen en bepalingen-methode, Delft, The Netherlands
- [2] Wellershoff, F. (2006) Nutzung der Verglasung zur Aussteifung von Gebäudehüllen, Shaker Verlag GmbH, Aachen, Germany
- [3] DIN 54 451, Schubspannungs-Gleitungsprüfung, Deutsches Institut für Normung, Berlin, Germany
- [4] ETAG 002 (2003), Guideline for European Technical Approval of Structural Sealant Glazing Systems, European Organisation for Technical Approvals, Brussels, Belgium
- [5] Huvener, E.M.P., Koggel, B.A. (2006), Tensile Shear Tests for the Determination of the Shear-Strain Diagram of several Adhesive Types, Eindhoven, The Netherlands
- [6] Holmes, M. (1961), Steel Frames with Brickwork and Concrete Filling, Proceedings of the Institution of Civil Engineers, vol. 19, pp. 473-478

